Dyes and Pigments 90 (2011) 139–145

Contents lists available at ScienceDirect

Dyes and Pigments

journal homepage: www.elsevier.com/locate/dyepig

Synthesis and characterization of solution-processable highly branched iridium (III) complex cored dendrimer based on tetraphenylsilane dendron for host-free green phosphorescent organic light emitting diodes

Seul-Ong Kim [a], Qinghua Zhao [a], K. Thangaraju [a], Jang Joo Kim [c], Yun-Hi Kim [b,*], Soon-Ki Kwon [a,*]

[a] School of Materials Science and Engineering, Engineering Research Institute (ERI), Gyeongsang National University, Jinju 660-701, Republic of Korea
[b] Department of Chemistry, and Research Institute of Natural Science (RINS), Gyeongsang National University, 900 Gajwa Jinju 660-701, Republic of Korea
[c] Department of Materials Sciences and Engineering, OLED Center, Seoul National University, Seoul 151-744, Republic of Korea

ARTICLE INFO

Article history:
Received 22 July 2010
Received in revised form
6 October 2010
Accepted 14 October 2010
Available online 19 November 2010

Keywords:
Highly branched dendrimer
Iridium(III) complex
Tetraphenylsilane dendron
Green emitter
Solution processed host-free phosphorescent OLEDs
Inhibited intermolecular interactions

ABSTRACT

Solution processable highly branched iridium(III) complex *fac*-tris(2-phenylpyridyl)iridium-cored dendrimer based on tetraphenylsilane dendron and 2-ethylhexyloxy surface groups was prepared. The structure of dendrimer was confirmed by nuclear magnetic resonance, mass and infrared studies. Thermogravimetric analysis and differential scanning calorimetry studies show the thermal stability ($\Delta T_{5\%}$) of 625 K with high glass transition temperature of 423 K. Photoluminescence studies of dendrimer showed the core emission at 516 nm in solution and at 521 nm in film, indicating the highly branched non-conjugated tetrahedral tetraphenylsilane dendrons around the core highly inhibit the intermolecular interactions between the cores in the film. The solution processed green emitting phosphorescent organic light emitting diodes based on dendrimer were fabricated and characterized. The device using host free dendrimer as emitter showed the external quantum efficiency of 0.4%. The results show the potential of this new type of dendritic emitting structure in highly efficient solution processed host-free green phosphorescent organic light emitting diodes.

1. Introduction

Organic light emitting diodes (OLEDs) have attracted a lot of attention due to their potential in full color flat panel displays as an efficient and low cost alternative to the widely used liquid-crystal display. When compared to fluorescent OLEDs where only singlet states emit the light and the efficiency is reduced because of triplet formation, phosphorescent OLEDs (PHOLEDs) are more efficient because of both singlet and triplets can be harvested for the light emission with close to 100% internal quantum efficiency [1–13]. Most of the phosphorescent devices were prepared by thermal evaporation process, making the fabrication process relatively complicated and expensive compared with the solution processed devices. In this context, solution-processable materials, which offer simple and cost-effective device fabrication process by spin-coating or ink-jet printing, could provide a better manufacturing process if simple device structures can also give high efficiencies. Although the efficiencies of phosphorescent small molecule based OLEDs are reasonably high, like in other organic light emitting materials, intermolecular interactions play a crucial role in the performances of such devices [14–18]. A number of methods such as most widely used method being blended the emissive material with a suitable host have been employed to control the intermolecular interactions [5,14,19–23]. However, in a blended system, whether evaporated or solution processed, there is always the issue of how evenly the guest is distributed in the host.

Intermolecular interactions can also be controlled very efficiently at the molecular level by using dendrimers [24–29]. Light emitting dendrimers are consisting of three parts: (i) a light emitting core, which is at the centre of the molecule and determines the light emitting properties, (ii) dendrons, which would generally be attached to the core chromophore and act as spacer that controls the interactions between cores in the solid state by increasing the distance between them, and (iii) surface groups, which are generally placed at the distal ends of the dendrons and control the processing properties of the molecules. In order to control the intermolecular interactions effectively in dendrimers, a strategy of increasing generation number has been utilized [25,26]. It has been reported that the intermolecular interactions have been significantly controlled for the dendrimers with highly efficient *fac*-tris(2-phenylpyridyl)iridium (III) [Ir(ppy)$_3$] cores, highly branched dendrons, and 2-ethylhexyloxy surface groups [30].

* Corresponding authors. Tel.: +82 55 751 5296; fax: +82 55 753 6311.
E-mail addresses: ykim@gnu.ac.kr (Y.-H. Kim), skwon@gnu.ac.kr (S.-K. Kwon).

0143-7208/$ – see front matter © 2010 Elsevier Ltd. All rights reserved.
doi:10.1016/j.dyepig.2010.10.005

Lo et al. reported that the increasing conjugation length of the ligand associated with the emissive metal-to-ligand charge transfer state resulted in the red-shifted emission of the core chromophore [27].

The purpose of the present work is to investigate an approach for controlling the intermolecular interactions between the core units in film state with reduced red-shift of the core emission, leading to be emitter for host-free device. In this approach, a highly branched well-known non-conjugated tetrahedral tetraphenylsilane dendron is attached to the each ligand of emissive core in the dendrimer (G1) to provide reduced interactions between core units in the film state with decreased conjugation length to the core as well as high band gap host [31]. PHOLEDs based on solution processed dendrimer (G1) consisting of (i) core: *fac*-tris(2-phenylpyridine)iridium [Ir(ppy)$_3$], (ii) dendrons: tetraphenylsilane, and (iii) surface groups: 2-ethylhexyloxy groups, which lead to high solubility, were fabricated and characterized. Photoluminescence and electroluminescence characteristics of the dendrimer (G1) and its devices were presented.

2. Experimental

2.1. Materials

Dibromobenzene, n-butyllithium, and 2-isopropoxy-3,3,4,4-tetramethyl-1,3,2-dioxaborolane were purchased from Aldrich. 2-Tri-n-butylstannylpyridine and 4-bromophenol was purchased from Lancaster. Tetrakis(triphenylphosphine)palladium was purchased from Strem. All reagents purchased commercially were used without further purification. Tetrahydrofuran (THF) and diethyl ether were dried over sodium/benzophenone.

2.2. Measurements

A Genesis II FT-IR spectrometer was used to record infrared (IR) spectra. ^{1}H-nuclear magnetic resonance (NMR) and ^{13}C-NMR spectra were recorded using Avance 300 and DRX 500 MHz NMR Bruker spectrometers and chemical shifts were reported in ppm units with tetramethylsilane as internal standard. Matrix-assisted laser desorption-ionization time-of-flight (MALDI-TOF) analysis was performed on an Applied Biosystems Voyager DE-STR MALDI-ToF (matrix; dithranol) mass spectrometer. Thermogravimetric analysis (TGA) was performed under nitrogen using a TA instrument 2050 thermogravimetric analyzer and the sample was heated at a heating rate of 283 K/min from 323 K to 1073 K. Differential scanning calorimeter (DSC) analysis was carried out under nitrogen environment using a TA instrument 2100 differential scanning calorimeter. The sample was heated at a heating rate of 283 K/min from 303 K to 573 K. UV–Visible (UV–Vis) absorption and photoluminescence (PL) spectra were recorded using Perkin Elmer LAMBDA-900 UV/VIS/NIR spectrophotometer and LS-50B luminescence spectrophotometer respectively. Cyclic voltammograms of the polymer films were recorded using an epsilon E3 cyclic voltammeter at room temperature in a 0.1 mol solution of tetrabutylammonium perchlorate (Bu_4NClO_4) in acetonitrile under nitrogen at a scan rate of 50 mV/s. A Pt wire was used as the counter electrode and an Ag/$AgNO_3$ electrode as reference electrode.

2.3. Synthesis

2.3.1. 2-(3-Bromophenyl)pyridine (**2**)

2-(Tri-n-butyl)stannylpyridine (31 g, 84 mmol) and 1,3-dibromobenzene (22 g, 93 mmol) were added to a 250 mL 2-neck flask with anhydrous toluene (200 mL) under nitrogen environment. After Pd(pph$_3$)$_4$ (0.48 g, 0.4 mmol) was added, the reaction mixture was refluxed for 24 h. Then the reaction mixture was poured into water and extracted with ethylacetate (EA). The product was purified by column using hexane: EA (20:1) as eluent. Yield: 14 g (71%). ^{1}H NMR ($CDCl_3$, ppm): 8.62 (d, 1H); 8.13 (s, 1H); 7.83 (d, 1H); 7.64 (t, 1H); 7.60 (t, 1H); 7.46 (d, 1H); 7.24 (t, 1H); 7.15 (t, 1H). MS (EI) *m*/*z*: 233 (M^+). Anal. Calcd for $C_{11}H_8BrN$: C, 56.44; H, 3.44; Found: C, 56.41; H, 3.47.

2.3.2. 2-[3-(4,4,5,5-tetramethyl-[1,3,2]dioxaborolan-2-yl)-phenyl]-pyridine (**3**)

N-butyllithium (19.54 g, 28 mL) was added to a solution of **2** (15 g, 64 mmol) in anhydrous tetrahydrofuran (THF) that had been cooled down using a dry ice/acetone bath under argon. The mixture was stirred at 195 K for 2 h and 2-isopropoxy-4,4,5,5-tetramethyl-1,3,2-dioxaborolane (13 g, 70 mmol) was added rapidly to the cold mixture. The reaction mixture was further stirred up at 195 K for 2 h, allowed to room temperature and stirred for 20 h. The reaction was quenched with water and extracted with EA. Then the product was purified by column using hexane: EA (20:1) as eluent. Yield: 6 g (33%). ^{1}H NMR ($CDCl_3$, ppm): 8.71 (m, 1H); 8.40 (m, 1H); 8.14 (m, 1H); 7.87 (m, 1H); 7.80 (m, 1H); 7.76 (m, 1H); 7.51 (m, 1H); 7.23 (m, 1H); 1.37 (s, 12H).

2.3.3. 1-Bromo-4-(2-ethylhexyloxy)benzene (**4**)

1- p-Bromophenol (17.3 g, 0.10 mol), 1-bromo-2-ethylhexane (44.4 g, 0.23 mol) and potassium carbonate (27.6 g, 0.20 mol) were mixed in acetone (100 mL). After refluxed for 24 h, the reaction mixture was allowed to cool to room temperature. Then the reaction mixture was poured into water and extracted with diethyl ether. After the combined organic material was washed with aqueous sodium hydroxide solution (10%, 100 mL) and water, the residue was distilled under reduced pressure to afford colorless oil. Yield: 23 g (75%). B.p. 131.8 °C/2 mmHg ^{1}H NMR ($CDCl_3$): 7.36 (d, 2H); 6.78 (d, 2H); 3.80 (d, 2H); 1.72 (m, 1H); 1.22 ~ 1.58 (m, 8H); 0.90 (m, 6H). MS (EI) *m*/*z*: 284 (M^+). Anal. Calcd for $C_{14}H_{21}BrO$: C, 58.95; H, 7.42; Found: C, 58.91; H, 7.44.

2.3.4. 2-[4-(2-Ethylhexyloxy)phenyl]-4,4,5,5-tetramethyl-[1,3,2]dioxaborolane (**5**)

N-butyllithium (3.8 mL, 5.66 mmol) was added to a solution of **4** (1.01 g, 3.54 mmol) in anhydrous tetrahydrofuran (7 mL) that was cooled by a dry ice/acetone bath under argon. The mixture was stirred at 195 K for 1 h. 2-Isopropoxy-4,4,5,5-tetramethyl-1,3,2-dioxaborolane (0.87 mL, 4.26 mmol) was added rapidly to the cold mixture and the mixture was stirred at 195 K for 2 h. Then, the mixture was allowed to room temperature and stirred for 8 h. Then the reaction was quenched with water and extracted with ethylacetate. The product was obtained by recrystallization in hexane. Yied: 0.8 g (69%). ^{1}H NMR ($CDCl_3$, ppm): 7.76 (d, 2H); 6.91 (d, 2H); 3.88 (m, 2H); 1.70–1.78 (m, 1H); 1.30–1.58 (m, 20H); 0.87–0.97 (m, 6H).

2.3.5. Tetrakis(4-bromophenyl)-silane (**6**)

Dibromobenzene (10 g, 40 mmol) and 100 mL of freshly dried diethyl ether were added to a 250 mL 2-necked flask. When the solution was cooled to 195 K using dry ice/acetone bath, *n*-BuLi (11.7 g, 40 mmol) was injected slowly and stirred for 2 h at 195 K. After the reaction mixture was maintained at 195 K, silicon tetrachloride ($SiCl_4$) (1.13 g, 6.7 mmol) was rapidly injected. Then the reaction mixture was stirred for 10 h at room temperature. After the reaction mixture was poured into water, the product was extracted with diethyl ether and dried over $MgSO_4$. The pure product was obtained by column-nchromatography using hexane as eluent. Yield: 3 g (67%). ^{1}H NMR ($CDCl_3$, ppm): 7.55 (d, 8H); 7.38 (d, 8H). MS (EI) *m*/*z*: 651 (M^+). Anal. Calcd for $C_{24}H_{16}Br_4Si$: C, 44.21; H, 2.47; Found: C, 44.17; H, 2.47.

2.3.6. 2-{4′-[Tris-(4-bromophenyl)-silanyl]-biphenyl-3-yl}-pyridine (**7**)

3 (1.72 g, 6.1 mmol) and **6** (8 g, 12.3 mmol) were mixed in THF and K_2CO_3 (2 mol, 15 mL). After tetrakis(triphenylphosphine)

palladium (0) ($Pd(pph_3)_4$) (0.15 g, 0.13 mmol) was added, the reaction mixture was refluxed for 24 h. Then, the reaction mixture was poured into 2 N HCl and extracted with ethylacetate. The pure product was obtained by column using hexane:EA as eluent. Yield: 2 g (45%). ^{1}H NMR ($CDCl_3$, ppm): 8.75 (d, 1H); 8.35 (s, 1H); 8.0 (d, 1H); 7.9 (d, 2H); 7.75 (m, 3H); 7.5 (m, 9H); 7.4 (m, 6H); 7.32 (m, 1H). MS (EI) *m/z*: 726 (M^+). Anal. Calcd for $C_{35}H_{24}Br_3NSi$: C, 57.87; H, 3.33; Found: C, 57.81; H, 3.37.

2.3.7. 2-(4′-{Tris-[4′-(2-ethylhexyloxy)-biphenyl-4-yl]-silanyl}-biphenyl-3-yl)-pyridine (8)

5 (1.8 g, 5.5 mmol) and **7** (1 g, 1.3 mmol) were mixed in THF with K_2CO_3 (2 mol, 15 mL). After tetrakis(triphenylphosphine)palladium (0) ($Pd(pph_3)_4$) (0.06 g, 0.07 mmol) was added, the reaction mixture was refluxed for 24 h. Then, the reaction mixture was poured into 2 N HCl and extracted with ethylacetate. The pure product was obtained by column using hexane: EA as eluent. Yield: 1.5 g (88%). ^{1}H NMR ($CDCl_3$, ppm): 8.8 (d, 1H); 8.38 (s, 1H); 8.1 (d, 1H); 7.92 ~ 7.72 (m, 14H); 7.6–7.7 (m, 12H); 7.3 (m, 1H); 7 (d, 6H). MS (FAB+) *m/z*: 1101. Anal. Calcd for $C_{77}H_{87}NO_3Si$: C, 83.88; H, 7.95. Found: C, 83.81; H, 7.99.

2.3.8. Dimer

A mixture of iridium chloride trihydrate ($IrCl_3$) (0.13 g, 0.43 mmol) and ligand (**8**) (1.5 g, 1.29 mmol) was added to a 3-neck 100 mL flask with 2-ethoxyethanol (21 mL) and water (7 mL) under nitrogen atmosphere. After the mixture was refluxed for 24 h, poured into water and extracted with dichoromethane. The pure product was obtained by column using hexane, hexane: EA, hexane: MC.

2.3.9. Dendrimer (G1)

A mixture of dimer, 1,4-diazabicyclo[2,2,2]octane (DABCO) (1.3 g, 12 mmol), ligand (**8**) (0.5 g, 0.5 mmol) in glycerol (25 mL) and tetra(ethylene glycol) (6 mL) were refluxed for 72 h. After the reaction mixture was poured into water and extracted with dichloromethane, the product was obtained by column using hexane: MC (1:1). Then, the yellow solid of dendrimer (**G1**) was obtained by PPT in MeOH. Yield: < 10%. ^{1}H-NMR ($CDCl_3$, ppm): 7.97 ~ 8.02 (m, 2H); 7.7 ~ 7.8 (m, 10H); 7.62 ~ 7.5 (m, 16H); 7.2 (m, 1H); 6.95 (d, 6H); 3.96 (d, 6H); 1.8 ~ 1.9 (m, 3H); 1.3 ~ 1.7 (m, 24H); 0.9 ~ 1.1 (m, 18H). FT-IR (KBr, cm^{-1}): 3065–3040 (aromatic C = C); 2994–2877 (aliphatic C–H); 1242 (C–O–C). MALDI-ToF MS (*m/z*): Calcd. For $C_{231}H_{258}IrN_3O_9Si_3$: 3496.8827, Found: 3496.7610.

2.4. Device fabrication

PHOLEDs based on synthesized dendrimer (G1) were fabricated using the configuration: indium-tin-oxide (ITO)/Poly(3,4-ethylenedioxythiophene)poly(styrenesulfonate) (PEDOT:PSS) (40 nm)/emissive layer (EML) (40 nm)/bathocuproine (BCP) (10 nm)/tris-(8-hydroxyquinoline)aluminum (Alq_3) (40 nm)/LiF (1 nm)/Al (100 nm). Prior to the deposition of organic layers, ITO substrates (anode) were degreased in acetone and IPA followed by the UV –ozone flux for 10 min. EML of Poly(N-vinylcarbazole) (PVK) (host) blended with dendrimer (G1) (guest emitter) with the concentration of 0.045 mmol/g for device A, 0.060 mmol/g for device B, 0.090 mmol/g for device C and EML of G1 neat film for device D were spin-coated on PEDOT:PSS thin film on ITO. BCP as hole blocking layer (HBL), Alq_3 as electron transport layer (ETL), LiF as electron injection layer and Al as cathode were deposited by thermal evaporation process under a vacuum of 6.6×10^{-6} Pa. The electroluminescence spectra were measured at a driving current of 1 mA cm^{-2}. The current density-voltage-luminescence (*J-V-L*) characteristics of PHOLEDs were carried out using Keithley 2400 source meter and Spectra Colorimeter PR650.

3. Results and discussion

The dendrimer (G1) was prepared as depicted in Fig. 1. The ligand (8) was prepared via manifold chemical reaction such as alkylation, Suzuki coupling reaction, etc as described below. 2-(3-Bromophenyl)pyridine was obtained from 2-tri-n-butylstannylpyridine and 1,3-dibromobenzene in the presence of $Pd(PPh_3)_4$ and toluene. Then, n-butyllithium and 2-isopropxy-4,4,5,5-tetramethyl-1,3,2-dioxaborolane were injected slowly to a solution of 2-(3-bromophenyl)pyridine and THF at 195 K to get the compound **3**. The compound **5** was prepared using the previous procedure [32]. Tetrachlorosilane and dibromobenzene were used to synthesize tetrakis(4-bromophenyl)-silane, it was further reacted with pyridine borate to give compound **7**. Similarly, the compound **7** was obtained by Suzuki coupling reaction with compound **5** to get the ligand **8**. The dendrimer (G1) with an iridium core was prepared by a modified, one-step approach. The iridium chloride trihydrate ($IrCl_3$) was treated with an excess of 1,4-diazabicyclo[2,2,2]octane (DABCO) and ligand 8 at 473 K for 72 h and served nitrogen atmosphere to give dendrimer (G1). Purification of the mixture by silica chromatography provided dendrimer (G1) as air-stable yellow powder. The obtained dendrimer (G1) showed high solubility due to the presence of 2-ethylhexyloxy surface groups. The structure of the dendrimer (G1) was confirmed by ^{1}H NMR, Mass and FT-IR spectroscopic studies. The thermo-gravimetric analysis (TGA) of dendrimer (G1) reveals that 5% weight-reduction temperatures ($\Delta T_{5\%}$) is 625 K. Especially, the differential scanning calorimetry (DSC) of dendrimer (G1) exhibits a distinct glass transition (Tg) around 423 K.

Fig. 2 shows UV–visible absorption and photoluminescence (PL) spectra of dendrimer (G1) and *fac*-tris(2-phenylpyridine)iridium [Ir$(ppy)_3$] in CH_2Cl_2 solution (10^{-5} mol solution) at the excitation wavelength of 381 nm. In the UV–vis absorption spectrum of dendrimer (G1), the absorption at around 280 nm assigned to π-π^* transitions of the core ligands is increased relative to that of Ir$(ppy)_3$ due to the biphenyl units within the dendron. The absorption at around 331 nm is due to the absorption of tetraphenylsilane dendron around the iridium complex core [33,24]. The absorption band with shoulders in the lower energy region spanning from 378 nm to 500 nm is attributed to spin-allowed and spin-forbidden metal-ligand charge transfer (MLCT) transitions of the Ir(III) complex [34–36]. From the PL spectra of dendrimer (G1) and Ir$(ppy)_3$, no changes were observed in the PL emission peak (emission wavelength = 516 nm) of dendrimer (G1) with slightly reduced full width at half maximum (FWHM) of 65 nm compared with that of Ir$(ppy)_3$ (emission wavelength = 516 nm, FWHM = 72 nm). This confirms the highly branched non-conjugated tetrahedral tetraphenylsilane dendron around the core provides the reduced conjugation length to core ligand in the dendrimer (G1) and inhibited intermolecular interactions between the core units [37]. The slightly reduced FWHM of emission spectrum of dendrimer (G1) compared with that of Ir$(ppy)_3$ also reveals the reduced interactions between the emissive core units in dendrimer (G1) in the solution. In Fig. 3, it is observed that the PL intensity (at emission wavelength of 516 nm) of dendrimer (G1) in solution is increased by two times compared with that of Ir$(ppy)_3$ when the excited wavelength was 331 nm, assigned to the dendron absorption (Fig. 2). This confirms that the energy absorbed by the dendrons could be efficiently transferred to the emissive core in the dendrimer (G1), leading to increased core emission. Fig. 4 shows the PL emission of dendrimer (G1) at 516 nm in solution and at 521 nm in film without the tail emission at higher wavelengths, which indicates that the core–core interactions are effectively controlled to a certain extent in the film by the highly branched non-conjugated tetrahedral tetraphenylsilane denrons around the

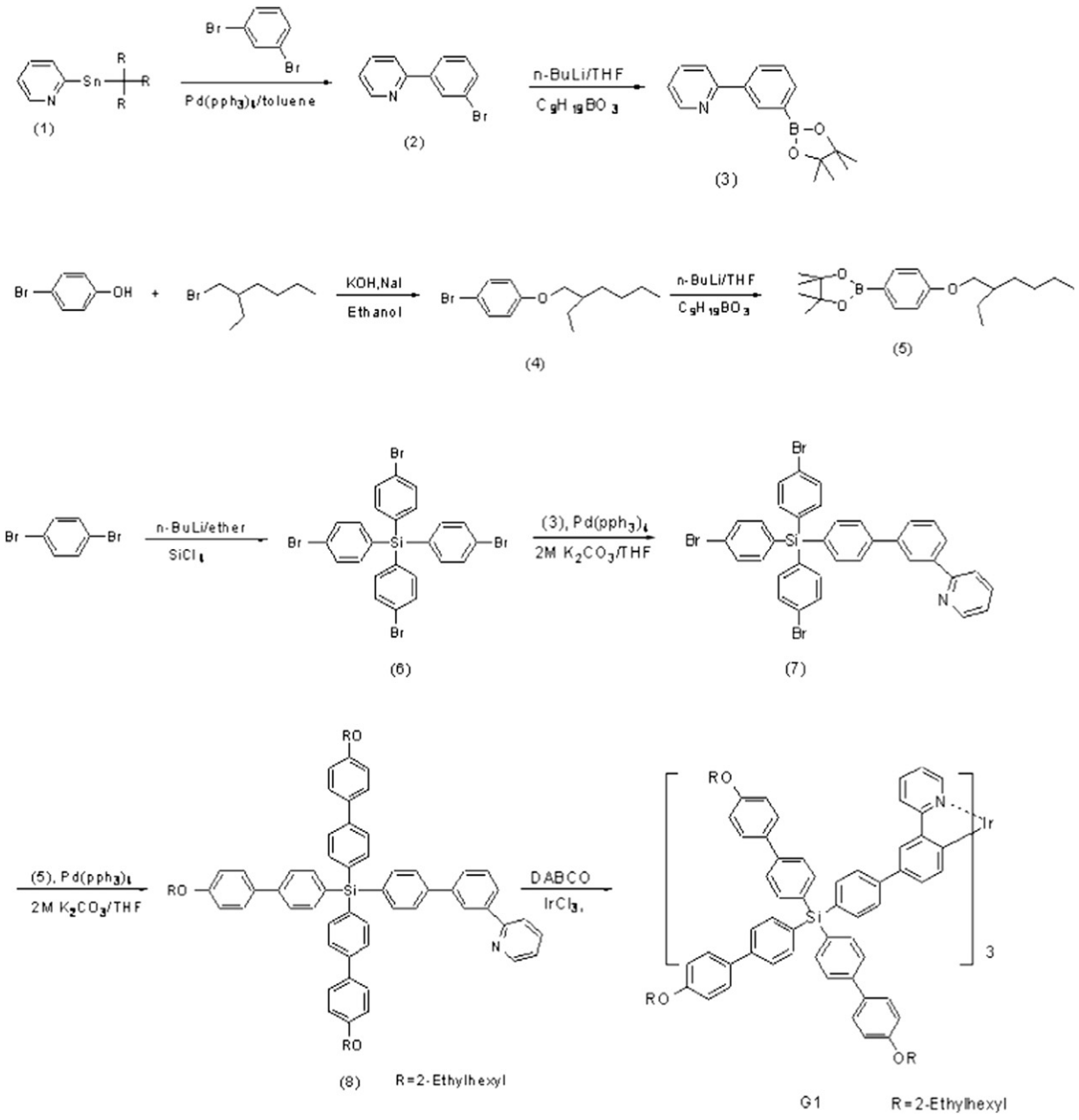

Fig. 1. Synthetic scheme of *fac*-tris(2-phenylpyridyl)iridium (III) cored dendrimer (G1).

core [38,39]. The PL emission of dendrimer (G1) film showed a slight red shift (5 nm) compared to that of solution. In general, a red shift of PL emission from solution to film was often observed, which is attributed either to the difference in the energy transfer processes between the film and the solution due to the presence of rotational conformers in the solution reducing the π-conjugation of the chromophores, or to the effect of the packing and local geometry of the materials [40]. The electrochemical properties of the dendrimer (G1) were investigated by cyclic-voltammogram (CV) studies. HOMO and LUMO energy levels were found to be 5.36 eV and 2.85 eV, respectively. The bandgap (2.51 eV) for the dendrimer (G1) was determined from the UV–visible absorption edge (495 nm) and this is slightly higher than that of $Ir(ppy)_3$ (2.46 eV) so as to be used as host as well as emitter in host-free devices [41].

The dendrimer (G1) has very good film and glass-forming properties for evaluating its electrophosphorescent ability. Solution processed PHOLED using the emissive layer (EML) of host-free dendrimer (G1) neat film was fabricated using the device configuration of ITO/PEDOT:PSS (40 nm)/emissive layer (EML) (40 nm)/BCP (10 nm)/tris-(8-hydroxyquinoline)aluminum (Alq_3) (40 nm)/LiF (1 nm)/Al (100 nm) (device D). The emissive layer was spin-coated from chloroform for the film thickness of 40 nm. The PEDOT:PSS layer was spin-coated for the thickness of 40 nm on ITO as hole injection and transport layer. The BCP and Alq_3 were used as the effective hole blocking layer and electron transporting layer, respectively. Indium tin oxide (ITO) was used as anode, while LiF/Al as cathode in the devices. The current density-voltage-luminescence (*J-V-L*) characteristics of the devices are shown in Fig. 5. Luminance efficiency (η_c)-current density (J)-power efficiency (η_p) characteristics of the devices are shown in Fig. 6. The device D showed the turn-on voltage of 4.7 V and maximum luminescence of 67 cd/m^2 at the operating voltage of 12.5V. The maximum device

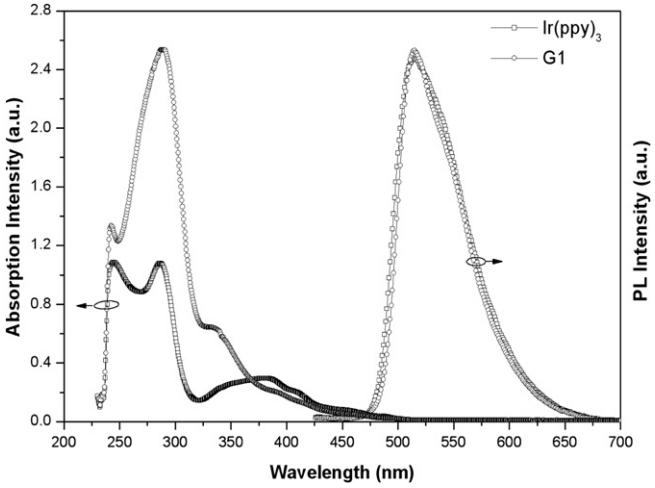

Fig. 2. UV–visible absorption and Photoluminescence spectra of dendrimer (G1) and Ir $(ppy)_3$ in CH_2Cl_2 at the excitation wavelength of 381 nm.

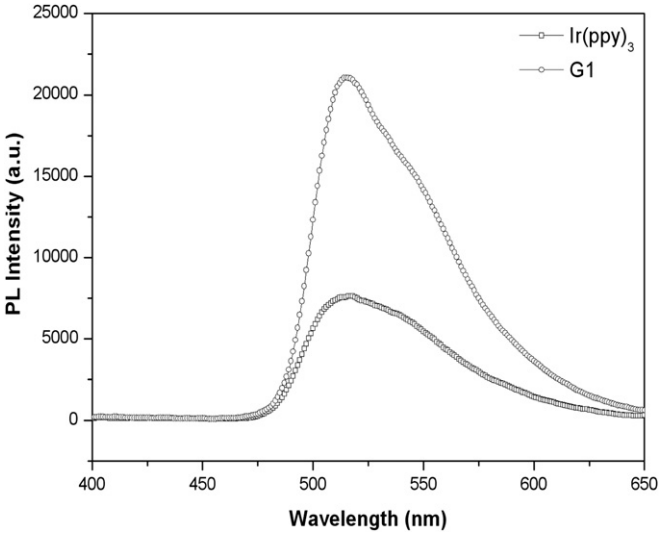

Fig. 3. Photoluminescence spectra of dendrimer (G1) and $Ir(ppy)_3$ in CH_2Cl_2 at the excitation wavelength of 331 nm.

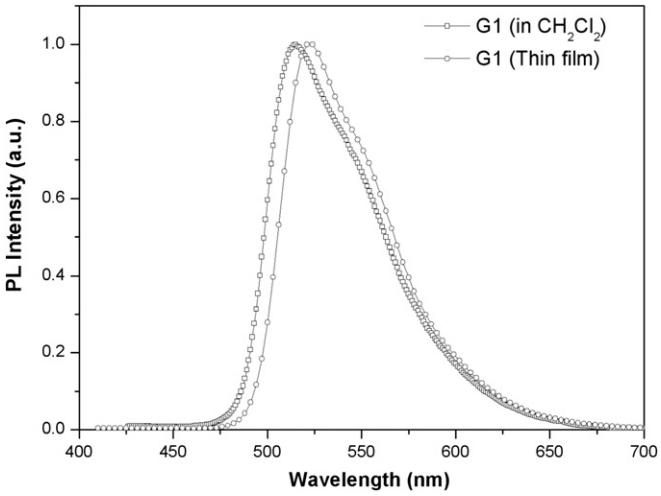

Fig. 4. Photoluminescence spectra of dendrimer (G1) in CH_2Cl_2 and film state at the excitation wavelength of 381 nm.

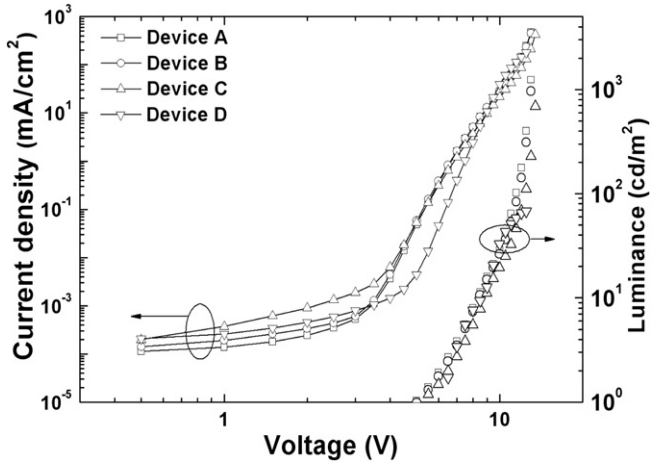

Fig. 5. Current density-voltage-luminescence (*J-V-L*) characteristics of devices A, B, C, and D.

efficiencies of 0.4%, 1.2 cd/A and 0.3 lm/W were observed for the device D with host-free dendrimer neat film as emitting layer. The electroluminescence (EL) spectra of the devices are shown in Fig. 7. The device D shows the electroluminescence peak at 522 nm, which is consistent with the PL emission of dendrimer (G1) in film, indicating EL and PL spectra are from the same excited state.

In order to compare the device performances of PHOLED using the EML of host-free dendrimer (G1) neat film, we fabricated similar structured-PHOLEDs using PVK: dendrimer (G1) blend as EML. The structure was ITO/PEDOT:PSS (40 nm)/PVK: dendrimer (G1) blend as EML (40 nm)/BCP (10 nm)/tris-(8-hydroxyquinoline) aluminum (Alq_3) (40 nm)/LiF (1 nm)/Al (100 nm). The dendrimer (G1) concentration of 0.045, 0.060 and 0.090 mmol/g of PVK was used for devices A, B and C, respectively. All three devices showed the similar performances. The devices based on PVK host showed the lower turn-on voltage (around 3.4 V) and higher current density compared with that of device D (4.7V), indicating the effective hole injection and transport properties of PVK host based devices. The maximum luminescence of 1237 cd/m^2 was reached for the device A. The device A showed the EL emission peak at 516 nm, which is consistent with the PL emission of dendrimer (G1)

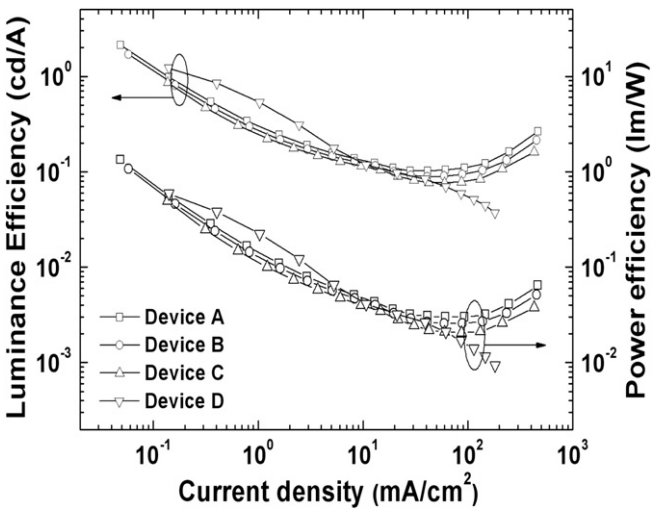

Fig. 6. Luminescence efficiency-current density-power efficiency characteristics of devices A, B, C and D.

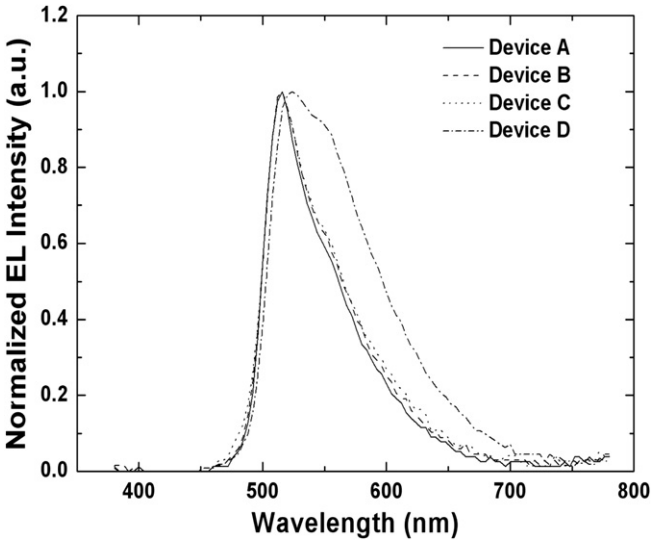

Fig. 7. Electroluminescence spectra of devices A, B, C and D.

in solution. This is slightly blue-shifted by 6 nm and narrowed compared with that (522 nm) of device D using the host-free dendrimer neat film as EML. This can be explained by the slightly different environment of dendrimer (G1) in PVK host compared with that of dendrimer (G1) in film state (40). It is observed that luminescence is increased at higher current densities for the devices A, B, and C compared with that of device D with host-free dendrimer neat film. The maximum device efficiencies of 0.7%, 2.1 cd/A and 1.3 lm/W were observed for the device A with dendrimer (G1) concentration of 0.045 mmol/g of PVK, while the device efficiencies of 0.3%, 0.5 cd/A and 0.9 lm/W were observed for device C with higher dendrimer concentration of 0.090 mmol/g of PVK. The device performances are decreasing upon increasing the dendrimer (G1) concentrations in the EML of devices B and C (Table 1tbl1tbl1) compared with that of device A without any change in the EL emission peak position with a small increase in the EL emission tail at higher wavelengths. This can be attributed to the fact that upon increasing dendrimer (G1) concentration in EML, aggregates seem to be increasing, which cause the long emission tail and act as trapping sites [42]. However, it has also been reported that the aggregates apparently are not operating as trapping sites as the current density is rather high and the local nanophase crystallization can occur in solid films of small amorphous molecule [42–44]. It is observed that the device efficiencies of the devices A, B, and C were unusually increasing at the higher current densities from 3×10^2 mA/cm^2, which can be related to the structural issues of the dendrimer (G1) in EML, according to the previous reports [42,43]. This could also in our case be the origin of such increase in the device performances of the devices A, B and C at higher current densities.

Table 1
The electroluminescence characteristics of the devices A, B, C and D.[a]

Device	Dendrimer(G1) in PVK as EML[b]	η_{ext} (%)	η_p (lm/W)	η_c (cd/A)
A	0.045	0.7	1.3	2.1
B	0.060	0.5	1.2	1.7
C	0.090	0.3	0.5	0.9
D	Neat film	0.4	0.6	1.2

[a] The device data for external quantum efficiency (η_{ext}), power efficiency (η_p) and luminance efficiency (η_c) are the maximum values of the corresponding device.
[b] The dendrimer(G1) concentration is mmol/g of PVK.

4. Conclusion

We prepared solution processable, highly branched *fac*-tris(2-phenylpyridyl)iridium (III) cored dendrimer (G1) and its structure was confirmed by ^{1}H NMR, mass and infrared spectroscopic studies. The dendrimer (G1) showed the high thermal stability ($\Delta T_{5\ \%}$) of 625 K with high Tg of 423 K. The highly branched non-conjugated tetrahedral tetraphenylsilane dendrons around the core unit effectively inhibited the intermolecular interactions between the core units in the dendrimer (G1) film. The device efficiencies of 0.4%, 1.2 cd/A and 0.3 lm/W were observed for the solution processed green emitting PHOLEDs using host-free dendrimer (G1) as emitter in the device structure of ITO/PEDOT:PSS/emissive layer/BCP/Alq_3/LiF/Al, while the device using PVK(host):dendrimer (G1) blend as emissive layer showed the maximum efficiencies of 0.7%, 2.1 cd/A and 1.3 lm/W. The results show that this new type of dendritic emitting structure has the potential in the highly efficient solution processed host-free green PHOLEDs.

Acknowledgement

This research was financially supported by MKE and KIAT through the Workforce Development Program in Strategic Technology, by Strategic Technology Under Ministry of Knowledge Economy of Korea and by Basic Science Research Program through the National Research Foundation of Korea (NRF) funded by the Ministry of Education, Science and Technology (2010-000826).

References

[1] Baldo MA, O'Brien DF, You Y, Shoustikov A, Sibley S, Thompson ME, et al. Highly efficient phosphorescent emission from organic electroluminescent devices. Nature 1998;395:151–4.
[2] Baldo MA, O'Brien DF, Thompson ME, Forrest SR. Excitonic singlet-triplet ratio in a semiconducting organic thin film. Physical Review B 1999;60:14422–8.
[3] Adachi C, Baldo MA, O'Brien DF, Thompson ME, Forrest SR. Nearly 100% internal phosphorescence efficiency in an organic light-emitting device. Journal of Applied Physics 2001;90:5048–50.
[4] Ikai M, Tokito S, Sakamoto Y, Suzuki T, Taga Y. Highly efficient phosphorescence from organic light-emitting devices with an exciton-block layer. Applied Physics Letters 2001;79:156–8.
[5] Lo S-C, Male NAH, Markham JPJ, Magennis SW, Burn PL, Salata OV, et al. Green phosphorescent dendrimer for light-emitting diodes. Advanced Materials 2002;14:975–9.
[6] Park Y-S, Kang J-W, Kang DM, Park J-W, Kim Y-H, Kwon S-K, et al. Efficient, color stable White organic light-emitting diode based on high energy level Yellowish-green Dopants. Advanced Materials 2008;20:61.
[7] Kang DM, Kang J-W, Park J-W, Jung SO, Lee S-H, Park H-D, et al. Iridium complexes with cyclometalated 2-cycloalkenyl-pyridine ligands as highly efficient emitters for organic light-emitting diodes. Advanced Materials 2008;20:2003–7.
[8] Leem D-S, Jung SO, Kim S-O, Park J-W, Kim JW, Park Y-S, et al. Highly efficient orange organic light-emitting diodes using a novel iridium complex with imide group-containing ligands. Journal of Materials Chemistry 2009;19:8824–8.
[9] Jung SO, Zhao Q, Park J-W, Kim S-O, Kim Y-H, Oh H-Y, et al. A green emitting iridium(III) complex with narrow emission band and its application to phosphorescence organic light-emitting diodes (OLEDs). Organic Electronics 2009;10:1066–73.
[10] Jung SO, Kang Y, Kim H-S, Kim Y-H, Lee C-L, Kim J-J, et al. Effect of substitution of methyl groups on the luminescence performance of $Ir^{(III)}$ complexes: preparation, structures, electrochemistry, photophysical properties and their applications in organic light-emitting diodes (OLEDs). European Journal of Inorganic Chemistry 2004;17:3415–23.
[11] Wong W-Y, Ho C-L. Functional metallophosphors for effective charge carrier injection/transport: new robust OLED materials with emerging applications. Journal of Materials Chemistry 2009;19:4457–82.
[12] Wong W-Y, Ho C-L. Heavy metal organometallic electrophosphors derived from multi-component chromophores. Coordination Chemistry Reviews 2009;253:1709–58.
[13] Zhou G, Wang Q, Ho C-L, Wong W-Y, Ma D, Wang L. Duplicating "sunlight" from simple WOLEDs for lighting applications. Chemical Communications; 2009:3574–6.
[14] Bera RN, Sakakibara Y, Abe S, Yase K, Tokumoto M. Time-resolved photoluminescence study on concentration quenching of a red emitting

tetraphenylchlorin dye for organic electroluminescent devices. Synthetic Metals 2005;150:9–13.
[15] Zhou G, Wang Q, Ho C-L, Wong W-Y, Ma D, Wang L, et al. Robust tris-cyclmetalated iridium(III) phosphors with ligands for effective charge carrier injection/transport: synthesis, redox, photophysical, and electrophosphorescent behavior. Asian Journal of Chemistry 2008;3:1830–41.
[16] Zhou G, Ho C-L, Wong W-Y, Wang Q, Ma D, Wang L, et al. Manipulating charge-transfer character with electron-withdrawing main-group moieties for the color tunning of iridium electrophosphors. Advanced Functional Materials 2008;18:499–511.
[17] Xia Z-Y, Xiao X, Su J-H, Chang C-S, Chen CH, Li D-L, et al. Low driving voltage and efficient orange–red phosphorescent organic light-emitting devices based on a benzotriazole iridium complex. Synthetic Metals 2009;159:1782–5.
[18] Xu Z, Li Y, Ma X, Gao X, Tian H. Synthesis and properties of iridium complexes based 1,3,4-oxadiazoles derivatives. Tetrahedron 2008;64:1860–7.
[19] Bera RN, Sakakibara Y, Tokumoto M, Saito K. Red-emitting organic electroluminescent devices with tetraphenylchlorin doped into a hole-transporting material. Japanese Journal of Applied Physics 2002;41:L391–3.
[20] Holmes RJ, Forrest SR, Tung Y-J, Kwong RC, Brown JJ, Garon S, et al. Blue organic electrophosphorescence using exhothermic host-guest energy transfer. Applied Physics Letters 2003;82:2422–4.
[21] Tokito S, Iijima T, Suzuri Y, Kita H, Tsuzuki T, Sato F. Confinement of triplet energy on phosphorescent molecules for highly-efficient organic blue-light-emitting devices. Applied Physics Letters 2003;83:569–71.
[22] Holmes RJ, D'Andrade BW, Forrest SR, Ren X, Li J, Thompson ME. Efficient, deep blue electrophosphorescence by guest charge trapping. Applied Physics Letters 2003;83:3818–20.
[23] Yang XH, Neher D. Polymer electrophosphorescence devices with high power conversion efficiencies. Applied Physics Letters 2004;84:2476.
[24] Namdas EB, Ruseckas A, Samuel IDW, Lo S-C, Burn PL. Photophysics of *fac*-tris (2-phenylpyridine) iridium(III) cored electroluminescent dendrimers in solution and films. Journal of Physical Chemistry B 2004;108:1570–7.
[25] Markham JPJ, Lo S-C, Magennis SW, Burn PL, Samuel IDW. High-efficiency green phosphorescence from spin-coated single-layer dendrimer light-emitting diodes. Applied Physics Letters 2002;80:2645–7.
[26] Lupton JM, Samuel IDW, Beavington R, Frampton MJ, Burn PL, Bassler H. Control of mobility in molecular organic semiconductors by dendrimer generation. Physical Review B 2001;63:155206–13.
[27] Lo S-C, Anthopoulos TD, Namdas EB, Burn PL, Samuel IDW. Encapsulated cores: host-free organic light-emitting diodes based on solution-processible electrophosphorescent dendrimers. Advanced Materials 2005;17:1945–8.
[28] Zhou G-J, Wong W-Y, Yao B, Xie Z, Wang L. Multifunctional metallophosphors with anti-triplet-triplet annihilation properties for solution-procecessable electroluminescent devices. Journal of Materials Chemistry 2008;18:1799–809.
[29] Zhou G, Wong W-Y, Yao B, Xie Z, Wang L. Triphenylamine-dendronized pure red iridium phosphors with superior OLED efficiency/color purity trade-offs. Angewandte Chemie International Edition 2007;46:1149–51.
[30] Bera RN, Cumpstey N, Burn PL, Samuel IDW. Highly branched phosphorescent dendrimers for efficient solution-processed organic light-emitting diodes. Advanced Functional Materirals 2007;17:1149–52.
[31] Yun H-K, Jeong H-C, Kim S-H, Yang K, Kwon S-K. High-purity-blue and high-efficiency electroluminescent devices based on Anthracene. Advanced Functional Materials 2005;15:1799–805.
[32] Ostrowski JC, Robinson MR, Heeger AJ, Bazan GC. Amorphous iridium complexes for electrophosphorescent light emitting devices. Chemical Communications 2002;7:784–5.
[33] Jae Jin Kim, Youngmin You, Young- Seo Park, Jang- Joo Kim, Soo Young Park. Dendritic Ir(III) complexes functionalized with triphenylsilylphenyl groups: synthesis, DFT calculation and comprehensive structure-property correlation. Journal of Materials Chemistry 2009;19:8347–59.
[34] Cumpstey N, Bera RN, Burn PL, Samuel IDW. Investigating the effect of steric crowding in phosphorescent dendrimers. Macromolecules 2005;38: 9564–70.
[35] Cho MJ, Jin JI, Choi DH, Kim YM, Park YW, Ju B-K. Phosphorescent, green-emitting Ir(III) complexes with carbazolyl-substituted 2-phenylpyridine ligands: effect of binding mode of the carbazole group on photoluminescence and electrophosphorescence. Dyes and Pigments 2009;83:218–24.
[36] Cho MJ, Jin JI, Choi DH, Yoon JH, Hong CS, Kim YM, et al. Tunable emission of polymer light emitting diodes bearing green-emitting Ir(III) complexes: the structural role of 9-((6-(4-fluorophenyl)pyridin-3-yl)methyl)-9H-carbazole ligands. Dyes and Pigments 2010;85:143–51.
[37] Lo S-C, Namdas EB, Burn PL, Samuel IDW. Synthesis and properties of highly efficient electroluminescent green phosphorescent iridium cored dendrimers. Macromolecules 2003;36:9721–30.
[38] Pei Q, Yang Y. Efficient photoluminescence and electroluminescence from a Soluble Polyfluorene. Journal of the American Chemical Society 1996;118: 7416–7.
[39] Kreyenschmidt M, Klarner G, Fuhrer T, Ashenhurst J, Karg S, Chen WD, et al. Thermally stable blue-light-emitting copolymers of poly(alkylfluorene). Macromolecules 1998;31:1099–103.
[40] Kim YH, Kwon SK, Yoo D, Rubner MF, Wrighton MS, Novel A. Bright blue electroluminescent polymer: a diphenylanthracene derivative. Chemistry of Materials 1997;9:2699–701.
[41] Lee JY. Effect of doping profile on the life time of green phosphorescent organic light emitting diodes. Applied Physics Letters 2006;89:153503–5.
[42] Slinker JD, Rivnay J, Moskowitz JB, Parker JS, Bernhard S, Abruna HD, et al. Electroluminescent devices from ionic transition metal complexes. Journal of Materials Chemistry 2001;17:2976–88.
[43] Blasini DR, Rivnay J, Smilgies DM, Slinker JD, Flores-Torres S, Abruna HD, et al. Observation of intermediate-range order in a nominally amorphous molecular semiconductor film. Journal of Materials Chemistry 2007;17:1458–61.
[44] Bolink HJ, Barea E, Costa RD, Coronado E, Sudhakar S, Zhen C, et al. Efficient blue emitting organic light emitting diodes based on fluorescent solution processable cyclic phosphazenes. Organic Electronics 2008;9:155–63.